THESIS FOR THE DEGREE OF LICENCIATE OF ENGINEERING

Legacy fostering the twins

Connecting the S/X and VGOS telescope network generations

REBEKKA HANDIRK

CHALMERS
UNIVERSITY OF TECHNOLOGY

Department of Space, Earth and Environment
Onsala Space Observatory
Research group for Space Geodesy and Geodynamics
Chalmers University of Technology
Gothenburg, Sweden 2024

Legacy fostering the twins
Connecting the S/X and VGOS telescope network generations
REBEKKA HANDIRK

Supervisor: Karine Le Bail, Department of Space, Earth and Environment
Examiner: Rüdiger Haas, Department of Space, Earth and Environment

Licenciate Thesis 2024
Department of Space, Earth and Environment
Onsala Space Observatory Division
Research group for Space Geodesy and Geodynamics
Chalmers University of Technology
SE-412 96 Gothenburg
Telephone +46 31 772 1000

Cover: The VGOS Onsala twin telescopes and the radome of the legacy S/X antenna. Copyright: Rebekka Handirk.

Typeset in LaTeX
Printed by Chalmers Reproservice
Gothenburg, Sweden 2024

Legacy fostering the twins
Connecting the S/X and VGOS telescope network generations
REBEKKA HANDIRK
Department of Space, Earth and Environment
Chalmers University of Technology

Abstract

With the VLBI Global Observing System (VGOS) being the next step in the development of geodetic Very Long Baseline Interferometry (VLBI), it is necessary to connect the new VGOS network to existing legacy S/X telescopes. Specially designed short-baseline interferometry sessions aim to obtain local-tie vectors between these telescope generations at observatories that have both legacy S/X and new generation VGOS telescopes.

At the Onsala Space Observatory (OSO), this is being done by short-baseline interferometry between the VGOS Onsala Twin Telescopes ONSA13SW and ONSA13NE, and the legacy antenna ONSALA60. Similarly, short-baseline interferometry sessions referred to as NYTIE have been performed at Ny-Ålesund, involving the VGOS telescope NYALE13S and the legacy S/X antenna NYALES20. In both cases, these dedicated experiments yielded station coordinates and baselines with mm or even sub-mm accuracy.

This thesis focuses on exploring the possibilities of connecting co-located radio telescopes with short-baseline interferometric measurements, specially in the cases of the observatories in Onsala and Ny-Ålesund.

Keywords: VLBI, S/X, VGOS, Local Ties, Space Geodesy

Acknowledgements

I would like to express my sincerest gratitude to my current and former supervisors, Dr. Karine Le Bail, Dr. Eskil Varenius, Dr. Tobias Nilsson, Prof. Emeritus Gunnar Elgered, and Dr. Maxime Mouyen, for their invaluable support and guidance. The countless hours of discussion, insightful feedback, and dedication to my development have equipped me with the knowledge and skills necessary to complete this thesis.
My deepest appreciation also goes to Prof. Rüdiger Haas, my examiner, for sharing his expertise and providing insightful suggestions that significantly improved the quality of my work.
To my fellow PhD candidates, thank you for creating a stimulating and supportive environment. Our shared experiences both during and after work have been a constant source of motivation. To the colleagues at the Onsala Space Observatory and at the Geodetic Earth Observatory Ny-Ålesund, thank you for a fantastic work environment and great collaboration.
A special thank you to Sara. I would not be where I am today without your dedication, encouragement and support.
Finally, to my family and friends, thank you for your unconditional love and support. This thesis is as much yours as it is mine, and I am forever grateful for your constant encouragement and belief in my abilities. Thank you for pushing me further than any of us could have expected.

Rebekka Handirk, Gothenburg, April 2024

Glossary

BKG Bundesamt für Kartografie und Geodäsie. 6

CRF Celestial Reference Frame. 6, 9

EOP Earth Orientation Parameters. 2, 6, 8
EVGA European VLBI Group for Geodesy and Astrometry. 21

GEON Geodetic Earth Observatory at Ny-Ålesund. xiii, 22, 23
GNSS Global Navigation Satellite System. 11, 14, 19, 24

IERS International Earth Rotation Service. 13–15
IVS International VLBI Service for Geodesy and Astrometry. xiii, 6, 8, 17–22, 26
IVS-CC IVS Coordinating Center. 6

LSA Least Squares Adjustment. 8, 9

NASA National Aeronautics and Space Administration. 6
NTSL Non-Tidal Station Loadings. 15
NYTIE Ny-Ålesund VLBI local-ties. 2, 20, 22, 24–26

OmC Observed minus Computed. 9
ONTIE Onsala VLBI local-ties. 2, 21, 24–26
OSO Onsala Space Observatory. xiii, 5, 9, 16, 21, 22

rcp right-handed circular polarised. 21, 22
RFI Radio-Frequency Interference. 19, 20

SET Solid Earth Tides. 14

TEC Total Electron Content. 13
TRF Terrestrial Reference Frame. 6, 9

VGOS VLBI Global Observing System. xiii, 2, 6, 8–10, 12, 13, 17, 19–22, 25
VLBA Very Long Baseline Array. 9
VLBI Very Long Baseline Interferometry. 1, 2, 5, 6, 8, 9, 11–14, 19, 21, 22, 25
VMF3 Vienna Mapping Function 3. 13

ZWD zenith wet delay. 8, 9

Contents

List of Figures

1
Introduction

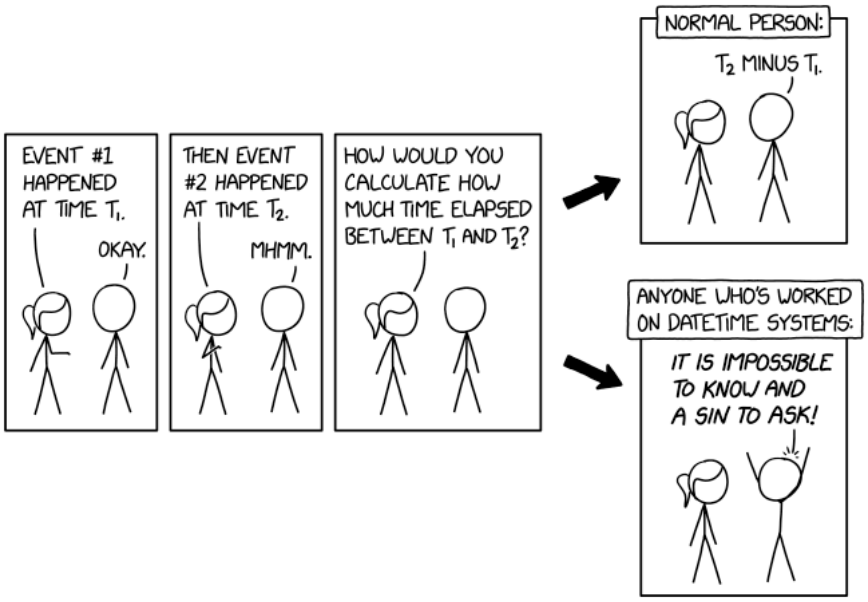

Figure 1.1: xkcd comic #2867[1]

With "DateTime systems", the comic above probably refers to programming, but the first thought, the first association certainly also depends on the reader's technical background. As a geodesist, my mind immediately goes to Very Long Baseline Interferometry (VLBI): A signal from a simultaneously observed radio source in space, such as a quasar, is received and recorded by several telescopes on Earth. The offset of the arrival times at the various stations is first used to calculate the distance between them, which in turn can provide information about the Earth's rotation, the Earth's orientation in space, tectonic plate movements and much more. The goal is to determine station coordinates with sub-mm accuracy, equivalent to a time stamp measurement accuracy of around 0.33 ps.
The term 'arrival time offset' refers to the time delay between T_2 and T_1. Unfortunately, calculating the time delay in VLBI is not as simple as subtracting T_1 from T_2. The delay is influenced by various factors, including atmospheric conditions,

[1] "#2867 DateTime" by Randall Munroe, retrieved from `https://xkcd.com/2867`. Used under Creative Commons Attribution-NonCommercial 2.5 license (`https://creativecommons.org/licenses/by-nc/2.5/`).

antenna structure deformations, earth rotation between T_1 and T_2, and others. Therefore, the last box could also be written as follows:

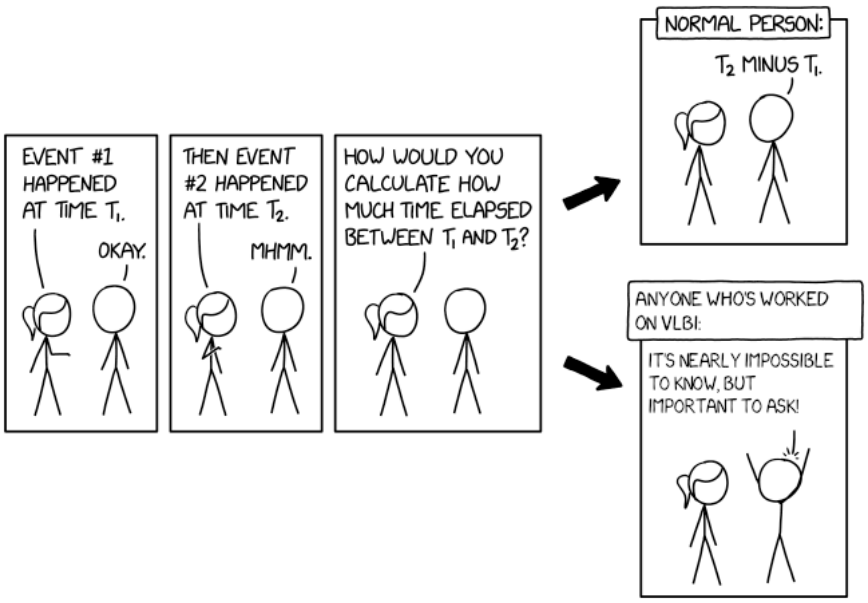

Figure 1.2: Adapted version of xkcd comic #2867.

. . . because it is the basic principle of VLBI to ask for the arrival times and their respective offsets.
As part of my research, I utilise this time offset to determine the distances between telescopes of different generations at the same observatory. This is where the title of my work comes into play: For decades, geodetic VLBI consisted of what is now called legacy S/X - a network of stations worldwide that regularly conduct joint observations to determine Earth Orientation Parameters (EOP), which take place in the S- and X-band of the radio spectrum. Recently, new generation VGOS telescopes have been built and put into operation, sometimes even at observatories with an existing S/X telescope. The new generation of telescopes is expected to eventually replace the S/X network. However, it is crucial to maintain the connection between the old and new telescopes to ensure that the reference to the decades of data already collected is not lost. This is where my work with the Onsala VLBI local-ties (ONTIE) and Ny-Ålesund VLBI local-ties (NYTIE) projects comes in: Two new telescopes - twins - have even been put into operation in both cases, that need to be related to their respective legacy S/X predecessors.

Outline of the thesis

This thesis focuses on VLBI-only local tie measurements between legacy S/X and VGOS telescopes at co-location sites. Chapter 2 provides an introduction to geodetic VLBI, including an explanation of interferometers and geodetic VLBI, an overview

of observables, experiment scheduling, and the time of arrival delay model. Chapter 3 presents the technical characteristics of the S/X and VGOS systems in more detail. Chapter 4 introduces the concept of local ties and presents specific research cases at the Onsala Space Observatory and the Geodetic Earth Observatory in Ny-Ålesund. The thesis concludes in Chapter 5, followed by a summary of the appended publications.

2

Very Long Baseline Interferometry

Our current radio geodetic and astronomic research can be traced back to the findings and research of two people: In 1932, radio engineer Karl Jansky was appointed by the Bell Phone telephone company to investigate interference signals in the short-wave band. He built a directional antenna and found that the signals reached a daily maximum that was shifted by four minutes each day. This shift led him to conclude that the source of the interfering signal must be outside the solar system. He also discovered that the interference was at a maximum when his antenna passed through the constellation of Sagittarius. We now know that the centre of the Milky Way (Sagittarius A*) lies in this direction. Jansky published his findings in 1933, but went mostly unnoticed in the scientific community at the time.
At the end of the 1930s, engineer Grote Reber built a parabolic antenna specifically devised to map the sky. He designed a parabolic dish antenna to act as a mirror: It concentrates the radiation at a focal point where it is directed to a receiver. Reber produced his first map of the sky, showing the intensity of cosmic radiation, and finally published his work in 1944. His idea of a parabolic antenna is still the basis of today's radio telescopes (Kellermann et al., 2020).
After the Second World War, military equipment was widely used for radio astronomy, for example at OSO, where in 1949 Olof Rydbeck acquired several 9 m dishes from Norway that had been left behind by the Germans (Lerner, 2012). In these early days of radio astronomy, image resolution was much lower than in optical astronomy. Therefore, arrays of telescopes were soon used to synthesise an aperture larger than the dish of a single telescope. These arrays became known as connected element interferometers, as they shared the clock standard used to time-tag the observations per antenna (Takahashi et al., 2000).
By the mid 1960s, the invention of atomic clocks enabled interferometers with baselines thousands of kilometers long. These yielded around 2 – 5 m accuracy in distance, and 1 arcsec for source positions (Sovers et al., 1998). Fast forward to today, there are now elaborate networks for both geodetic and astronomical VLBI, reaching sub-mm accuracy for station positions and creating images with much higher resolution that optical telescopes would allow.

2.1 What is an interferometer?

When observing from a single dish, the angular resolution at a given frequency is proportional to the inverse of the diameter of the antenna. Thus, when bound to

a certain frequency, the angular resolution fully depends on the diameter. To overcome this limitation, an interferometer observes the same source with several dishes simultaneously. This mimics a large antenna with a diameter that corresponds to the baseline length between the telescopes. The signals from each involved telescope are correlated to find the time delay of the recorded signal per station. To follow up, there are three concepts in VLBI: Astronomical VLBI uses the time delay to investigate the radio source, while geodetic VLBI observes "stable" sources that are assumed to remain fixed over time and frequency and uses the time delay to estimate station coordinates. Additionally, atmospheric and clock parameters can be obtained from analysis.
It is important to note that with VGOS we see even clearer that stability assumptions are not fully true and some sources do change over time and look different at different frequencies.
The third type, the astrometric VLBI aims at obtaining highly accurate radio source positions. It can also yield station positions, however not as accurately as geodetic VLBI, and atmospheric parameters are not of interest during analysis.

2.2 Geodetic VLBI

The primary interest of geodetic VLBI is the determination of Earth rotation and Earth orientation in space, which is commonly summarised by the EOP, as well as the facilitation of Celestial Reference Frame (CRF) and Terrestrial Reference Frame (TRF). The EOP consist of five parameters representing nutation, precession, polar motion, and UT1-UTC. The latter describes the difference between mean solar time at 0° longitude and the internationally agreed Coordinated Universal Time scale which is based on atomic clocks.
Through the EOP, geodetic VLBI thus provides the connection of the TRF and the CRF.

Coordination for geodetic VLBI is organised by the IVS (Nothnagel et al., 2017). The IVS Coordinating Center (IVS-CC) organises the master schedule, i. e. when experiments are to take place and which stations are to participate, depending on their respective availabilities. Further, the IVS-CC allocates the task of experiment scheduling to IVS members, appoints correlation and analysis centres, and finally provides the EOP and more as official products[1] via cooperating data centres hosted by National Aeronautics and Space Administration (NASA) Goddard Space Flight Center, the Bundesamt für Kartografie und Geodäsie (BKG), Germany's national mapping agency, and the Paris Observatory.

2.3 Observables

Fig. 2.1 illustrates the fundamental concept of VLBI, which involves observing a radio source simultaneously with at least two telescopes. The observed sources

[1] https://ivscc.gsfc.nasa.gov/products-data/products.html

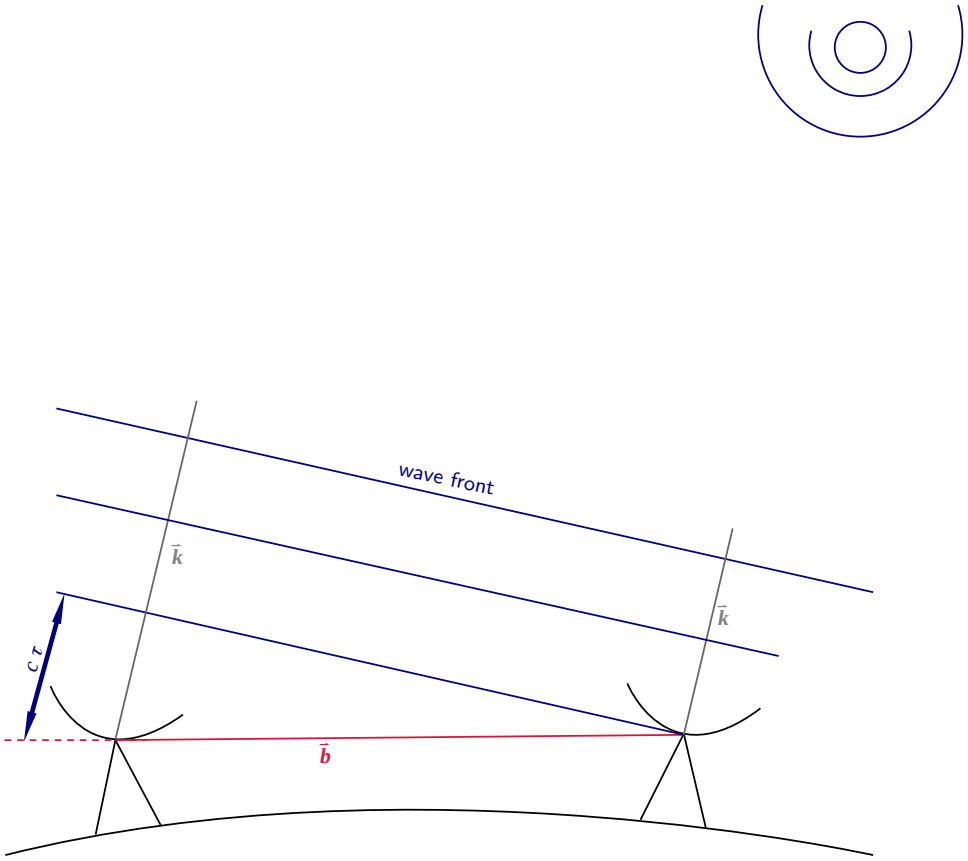

Figure 2.1: Schematic representation of a VLBI observation with 2 telescopes: Wave fronts from a radio source reach the telescopes. Due to the large distance of the source the wave fronts are planar and parallel when reaching. The recorded signals at the participating telescopes are shifted by the delay τ. The telescopes span the baseline $\vec{b}$, and the direction to the radio source is given by the vector $\vec{k}$ for each telescope.

are located at such great distances that the wave fronts can be assumed planar when reaching the telescopes. A wave front may reach one of the telescopes before the other, resulting in the time delay discussed in Section 2.1. In practice, the signal passes through a low-noise amplifier and a down-conversion stage before being recorded at the respective station. The main observable, the time delay τ, is later obtained in the correlation process of two (or more) signals.
The purely geometric time delay depends not only on the baseline length, but also on polar motion, nutation, and precession. Also, Earth rotation needs to be accounted for because station 2 moves further between the arrival of the signal at station 1 and station 2, i. e. the baseline vector actually changes during the process of recording what should be the same signal. This effect is known as abberation.
Post-correlation steps and analysis (usually a Least Squares Adjustment (LSA)) are used to find e. g. station coordinates and velocities, EOP, the tropospheric zenith wet delay (ZWD), and clock parameters.

2.4 The IVS observing program

Scheduling for geodetic VLBI is done with dedicated scheduling software packages. Most common are *sked* (Gipson, 2018) and *VieSched++* (Schartner, 2021). Depending on the actual goal of a specific session, priority might be given to good sky coverage, network volume, certain properties of the sources to be observed, the number of observations, idle time of the telescopes involved, etc.

As Chapter 3 explains in more detail, geodetic VLBI currently consists of two different networks. The older one is usually referred to as "legacy" or "S/X", while the newer one is commonly called "VGOS". The name "S/X" is a reference to the covered frequency bands by the antennas involved.

The IVS observing program is dominated by Rapid Turnaround sessions and several Intensive sessions. Rapid Turnarounds are typically 24 h long, while Intensives usually last only 1 h. The main goal of these sessions is to determine the EOP. Intensives are particularly used to establish a daily determination of UT1-UTC, the most critical EOP for other space applications, as it is needed for orbit determination (and can only be determined by VLBI).
For the legacy network, Rapid Turnaround sessions are IVS-R1 and IVS-R4. In the future, the VO sessions for the VGOS network are expected to become the equivalent of today's Rapid Turnarounds R1 and R4. The Intensive sessions are abbreviated as IVS-INTx resp. VGOS-INTx, with x as a placeholder for the various particular types, irrespective of the network.
IVS-R1 and IVS-R4 experiments happen on a weekly basis, and include usually 8 – 14 stations (Thomas et al., 2024). VOs are supposed to be conducted every week, with the goal of building up a network with infrastructure able to observe 24/7. However, even a cadence of one experiment per week in addition to the other non-VGOS experiments has repeatedly created large backlogs at the correlator and analysis centres. The processing delays are mainly due to the logistic challenges present with transferring the large amounts of data (typically 1 TB per hour per

VGOS telescope) from the observatories to the correlation centres, and due to the amount of time it takes to correlate the data. The current observation cycle is therefor one session per week for the duration of three weeks, followed by a fourth week without any VO.
Further, less frequent sessions are dedicated to particular research questions (thus referred to as R&D, research and development, resp. VR for the S/X and the VGOS network), the strengthening of the determination of TRF and CRF, or to a specified subset of stations such as the Very Long Baseline Array (VLBA).
In the course of this thesis, the above mentioned session types will be referred to as R1, R4, RD (IVS research and development sessions), and RDV (research and development dedicated specifically to the VLBA).

2.5 Delay model

The observed time delay can be represented as $\tau = t_2 - t_1$, where t_1 and t_2 are the arrival times of the signal at stations 1 and 2, respectively. It is important to note that this equation assumes an ideal scenario, where the baseline is fixed and the signal travels exclusively through a vacuum. The baseline vector must be adjusted to either t_1 or t_2.
To ensure accuracy, it is important to account for the error budget mentioned in the subsections below. After this, one calculates the Observed minus Computed (OmC) in a LSA with output parameters such as station coordinates, source coordinates, clock polynomial, and ZWD. It is important to note that the LSA is non-linear and therefore requires a-priori values. The delay in the radio signal can be attributed to various factors:

$$\tau_{obs} = \tau_{geom} + \tau_{instr} + \tau_{source} + \tau_{atmo} + \tau_{other} + \epsilon \tag{2.1}$$

The delay due to the geometry of the system, which includes the position of the radio source and of the telescope, is denoted by τ_{geom}. τ_{instr} relates to the entire telescope system, encompassing the antenna, cables, recording system, and clock. The delay caused by the structure of the radio source is denoted by τ_{source}. Additionally, there are atmospheric delays caused by the neutral atmosphere and the ionosphere, summarised and denoted by τ_{atmo}. This is recognised as one of the biggest error sources in VLBI. τ_{other} relates to further effects such as relativistic effects, and ϵ to the overall noise.
The individual delays are discussed in more detail in the following subsections. For all of them, except for the source structure, corrections are implemented in the analysis software ASCoT (Artz et al., 2016), used at OSO, similar as in other analysis software packages. Traditionally, geodetic VLBI observations have been scheduled to target point-like sources, i. e. sources that do not show significant structure. Therefore, corrections for source structure are not utilised in the geodetic VLBI data analysis, although efforts are made to observe sources that exhibit minimal structure.

Group and phase delays Given that geodetic VLBI is typically observed across multiple frequency bands, there are two distinct approaches to analysing the data. On the one hand, the time offset can be observed individually on each frequency. This type is usually referred to as "phase delay". Phase delays are particularly precise, but unfortunately their evaluation is characterised by only being possible for short baselines, which is mostly caused by the impact of the neutral atmosphere and ionosphere on the phase ambiguities on longer baselines. This is distinct from the approach taken with group delays, where all frequencies within a given band are analysed collectively, where one tries only to align the slope of the phase vs. frequency function, but not the actual phase offset. Fig. 2.2 illustrates the concept of group delay.

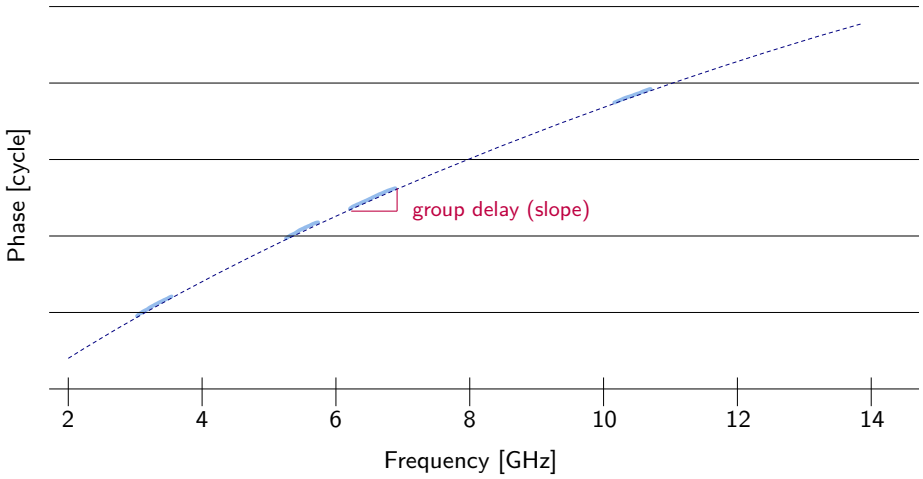

Figure 2.2: Example sketch of the phase vs. frequency function. Darker patches show the approximate positions of the VGOS observation bands (Kallunki et al., 2023) in the frequency spectrum.

2.5.1 Instrumentation related error budget τ_{instr}

The error sources mentioned in this section can be related to impacts on the antenna reference point.

2.5.1.1 Gravitational deformation

The large structure of the telescope dish deforms under its own weight which affects the signal path length by changing the focal length of the antenna. This effect is dependent on the elevation angle, usually approximately proportional to $\sin(El)$ (Sovers et al., 1998), with El the elevation angle of the telescope. While some antennas can move the subreflector to compensate, this is not desirable for geodetic measurements. This compensation method only works for astronomical VLBI, as it

alters the signal path length during observation.
The size of the effect depends on each individual telescope. The Effelsberg telescope, which is one of the largest with its 100 m diameter, experiences a difference of nearly 100 mm difference in total path length when observing at 0° or 90° elevation (Artz et al., 2014).
General models are available (Artz et al., 2014) to describe gravitational deformation. For some telescopes, specified models are available, such as for ONSALA60 (Nothnagel et al., 2019).

2.5.1.2 Thermal deformation

All materials expand with a certain temperature coefficient. This expansion displaces the antenna reference point vertically, which can be significant for larger antennas, sometimes resulting in displacements of several millimetres (Sovers et al., 1998). Nothnagel (2008) states that most VLBI telescopes can be expected to show height variations of 4 – 6 mm due to thermal deformation. However, he also notes that e. g. the Effelsberg telescope may experience height variations of about 20 mm due to the seasonal temperature changes.
As for the gravitational deformation, general models are available (Nothnagel, 2008), and for some telescopes, there are even specified models such as ONSALA60 (Nothnagel et al., 2019).

2.5.1.3 Clock

To properly correlate observation data from the same source using at least two different telescopes, a good initial guess of the delay between the telescopes involved is essential. This requires the use of highly accurate clocks with both long and short term stability. Clivati et al. (2017) emphasises the importance of spectral purity in clocks, as phase noise scales with N^2 when multiplications are concatenated (where N is the ratio between the frequencies of the radio signal and the clock).
Currently, atomic clocks are the most suitable for meeting these requirements. Atomic clocks are solely used to generate regular pulses for the local oscillator. Global Navigation Satellite System (GNSS) timing is then used to label the pulses with a time stamp. This is because GNSS timing averages alone are not accurate enough. Atomic clocks provide the pulses but not the time stamp, or name, of each pulse as the time stamps would not be consistent due to the clock drift.

2.5.1.4 Feed rotation

Feed rotation, sometimes also referred to as “parallactic angle”, comes into play when the receiver rotates relative to the sky polarisation axes during the experiment, which alters the antenna feed’s orientation with respect to a radio source.
In the case of a circular polarised receiver the feed rotation means a phase-change in the circular basis. For linear polarised receivers the effect is more complicated, because the rotation means that emission in the X-basis will eventually rotate to the Y-basis.
Sovers et al. (1998) gives an equation to account for this effect, which impacts

mostly alt-az-mount telescopes when observing with a circular polarised receiver. For equatorially mounted telescopes with a circular polarised receiver they report the effect to be close to zero.
In the case of linear polarised receivers, as typically used in VGOS equipment, other means of correction have been developed, e. g. polconvert (Martí-Vidal et al., 2016).

2.5.2 Source structure related error budget τ_{source}

As already mentioned in Section 2.1, geodetic VLBI assumes the radio sources to be stable. Ideally, they would even be point-like with no structure whatsoever. However, in most cases the observed sources are not point-shaped, they may in fact consist of two radio sources that are very close to each other but still need to be treated separately. This would create the problematic question of finding the right single delay.
While astronomers routinely produce images of many radio sources, they cannot monitor all sources interesting for geodetic VLBI. In consequence, there is no broad, regular update available, which led geodesists to avoid the problem by chosing the most point-like sources for observations while leaving out all others.
Also, point-like sources do unfortunately not necessarily stay point-shaped throughout their life time. Even if astronomers were providing geodetic VLBI with images of radio sources, they would therefore constantly have to monitor and update their catalog of images.
With the advent of VGOS the quality of geodetic observations has increased which eventually could potentially enable the provision of full-polarisation structure maps and flux density measurements of all geodetic-VLBI sources. A first successful attempt of monitoring source flux with VGOS telescopes was published by Varenius et al. (2022). Also, first attempts have been made to develop corrections for source structure. Especially VGOS could profit from source structure corrections, since it is one of the strongest effects on the measurements (Anderson and Xu, 2018).

2.5.3 Signal propagation related error budget τ_{atmo}

Error budget related to the signal propagation stems mostly from the effect of the signals travelling through Earth's atmosphere (Petit and Luzum, 2010), which is one of the major impacts on the measurements.

2.5.3.1 Delay caused by the neutral atmosphere

Fermat's principle states that light always takes the path with the shortest transit time. If the path leads through any medium with an incidence angle different from 0°, the optical path does not correspond to the geometrically shortest path. The effects of the delay of the neutral atmosphere are caused both by the troposphere and the stratosphere. Earth's troposphere is a non-dispersive medium for microwaves. Its refraction index depends on temperature, pressure, humidity, compressibility and characeteristics of the contained molecules. Modelling of the tropospheric effect is usually separated into two parts: the hydrostatic part and the wet part. The hydrostatic part represents ca. 90 % of the total effect and can be modelled quite

well. The wet part, however, displays strong spatial and temporal variations and is very difficult to model. For this reason, the VLBI observations are usually used to estimate the wet part directly, since the observations are typically made at many different telescope elevation angles. Petit and Luzum (2010) report the effects of the hydrostatic part to amount to about 2.3 m, and 10 – 150 mm for the wet part, which makes it one of the largest error sources in geodetic VLBI (Nilsson and Haas, 2010).
The International Earth Rotation Service (IERS) recommends following the standard model introduced for the hydrostatic part by Saastamoinen in 1972 and points out improved mapping functions for both the dry and the wet part based on Herring's general form from 1992 (Petit and Luzum, 2010). Mapping functions are necessary to get the actual slant delay in the direction of the source. Typically, a slant delay is computed by multiplying the zenith delay with a mapping function and by adding some gradients. In VLBI, the Vienna Mapping Function 3 (VMF3) (Böhm and Schuh, 2004; Landskron and Böhm, 2018) is often used.

2.5.3.2 Ionospheric delay

Earth's ionosphere is a dispersive medium, i. e. its refraction index depends on the signal frequency. To correct for its effect on the received signal, the phase refraction index and the group refraction index are needed. The most important parameter is the number of free electrons, measured as Total Electron Content (TEC) where 1 TEC unit corresponds to 10^{16} electrons/m^2 (Hofmann-Wellenhof et al., 2008; Sovers et al., 1998). The vertical TEC (VTEC) depends on the local time of the day (more radiation – more free electrons). Since the ion production rate peaks at roughly 350 km height, a common approach is to use a single layer model that reduces all TEC to a single layer where free electrons are concentrated (Hofmann-Wellenhof et al., 2008).
The ionospheric effect is best dealt with when observing two different, well-separated frequency bands simultaneously. This gives the possibility to calculate what is called an ionosphere-free linear combination (Sovers et al., 1998). For the next generation VGOS the ionospheric correction is instead included in the fringe-fitting process.
Petit and Luzum (2010) report the effect to amount to a few picoseconds for VLBI measurements.

2.5.4 Other delays τ_{other}

Other delays include e. g. the Shapiro delay. The Shapiro delay is the time delay caused by the gravitational field of the Earth and other celestial bodies. Petit and Luzum (2010) also provide the necessary formula for this effect. The effect is first calculated individually for each body and the individual results are then totalled. The effect can be in the order of several hundred picoseconds.
For observations near the sun, the IERS conventions (Petit and Luzum, 2010) recommend an additional relativistic correction.

2.5.5 Station movement

The earth's crust is subject to regular displacements, which contain tidal and non-tidal components. These displacements can be described using geophysical models (Petit and Luzum, 2010), and in particular must be taken into account in the VLBI analysis model.

Tides on Earth are caused by the different forces of attraction of other celestial bodies on different regions of the Earth. The part of the Earth that is closest to the external body is attracted with greater force than parts that are further away. This causes the Earth to deform in the direction of the influencing body.
The moon exerts the greatest influence on the Earth, followed by the Sun. In the past, tides were measured using tide gauges and gravimeters. Nowadays, however, space geodetic methods are also used: VLBI, GNSS and correction values from satellite orbit calculations show the influence of degree 2 tides on a global scale. As VLBI observations cannot be carried out everywhere, GNSS data is often used (Agnew, 2007).
Various geophysical models are used to calculate the tidal effects on stations on Earth. These consider different influences individually, so that the models can only provide as complete an impression as possible in combination with each other.

Solid Earth Tides When modelling the Solid Earth Tides (SET), a spherical Earth body without oceans is assumed and it is calculated how this would behave under the influence of external bodies (Agnew, 2007). For modelling purposes, it is assumed that the Earth rotates in its orbit and around its own axis.
Spherical-harmonic tidal models of degree n and order m are obtained from the modelling. In addition to degree and order, their values also depend on the latitude of the point for which they are calculated, as the Earth is treated as a rotational ellipsoid and the Coriolis force must be taken into account. The exact formulae for the calculation are listed in the IERS Conventions 2010 (Petit and Luzum, 2010).
SET show the largest impact on station coordinates of the tidal loading effects. They account for several decimeter in station movement (Petit and Luzum, 2010).

Ocean Loading As already mentioned, the SET refer to an Earth modelled without oceans. However, the displacement of ocean masses also leads to deformation. Regional and local conditions play an important role in their modelling, which is why the effect is calculated using a grid. The surcharge is determined by integrating the tidal height including a weight function. The IERS recommends the use of TPX7.2 (a model obtained from tide gauge measurements and TOPEX/Poseidon data) or FES2004 (a hydrodynamic model obtained from altimetry data) or older models, if these are useful due to internal consistency with other calculations (Petit and Luzum, 2010). Different periods are also superimposed in the ocean loadings. However, the effect is an order of magnitude smaller than that of the SET.

Solid Earth Pole Tides An additional effect of about 2 cm in the vertical coordinate component is created by the fact that the Earth's axis of rotation moves

around an imaginary point. This rotation is dominated by a 12-month and a 14-month period (known as the Chandler period). The speed of the Earth's rotation also influences the effects. The IERS also provides the necessary formulae for modelling (Petit and Luzum, 2010).

Ocean Pole Loading Ocean pole tides arise because the polar movement in turn also leads to a shift in the ocean masses. The IERS also provides the formulae required for this modelling (Petit and Luzum, 2010). As with the polar motion, a sinusoidal periodicity characterises the model. Since the trigger is the polar motion, the annual and Chandler periods also dominate here. The effect amounts to ca. 2 mm for the vertical coordinate component.

Atmospheric Loading Like the ocean masses, the atmospheric masses also deform the Earth. In this case, the influence can be seen almost exclusively in the station's Up component, since the air masses mainly press directly on the Earth's surface from above. In the IERS Conventions 2010 it is recommended to use an empirical model that describes diurnal and semidiurnal variations. According to Petit and Luzum (2010), the amplitude of the effect due to diurnal and semi-diurnal atmospheric loads is on the order of several millimeters.

Non-Tidal Station Loading Oceans and the atmosphere exert a load on the stations not only through their tides, but also independently of the tides. These so-called Non-Tidal Station Loadings (NTSL) include loads from the atmosphere (non-tidal atmospheric loading), oceans (non-tidal ocean loading and non-tidal sea level loading) and hydrology, i.e. water masses on the continents (non-tidal hydrological loading).
Tidal deformations are caused by gravitational forces, which in the case of the Earth are primarily exerted by the moon and the sun, and by centrifugal forces caused by the Earth's rotation. Non-tidal deformations, on the other hand, result from locally limited and irregular changes in atmospheric pressure or mass redistributions of water (ocean and hydrology). The German Research Centre for Geosciences (GFZ), for example, provides models for correction (Deutsches GeoForschungsZentrum, 2019). Each of the models relates to one of the four components mentioned above, so that the models only depict the full effect in combination with each other.

Station movement due to plate tectonics The Earth's mantle contains convection currents of heating and cooling magma, which move the tectonic plates. This causes the observatories to move with them and this movement is visible, for example, in the terrestrial coordinate system, whereby the speed and direction of movement differ from plate to plate. The slowest movements are only a few millimetres per year, while the fastest plate moves at more than 110 mm per year (Zhang et al., 2017).
Fig. 2.3 displays how plate tectonics have enlarged the baseline between the Onsala Space Observatory and Haystack Observatory from 1980 to 2022 at a rate of about 16 mm per year.

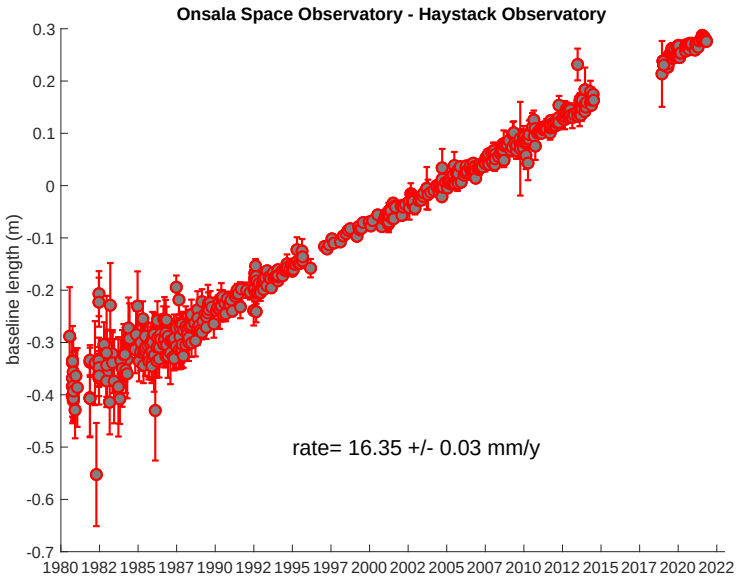

Figure 2.3: Baseline length between the Onsala Space Observatory and Haystack Observatory from 1980 to 2022[2].

Glacial Isostatic Adjustment During the ice ages, huge amounts of ice masses pressed the Earth's crust deeper into the mantle. Even tens of thousands of years after the last ice age, the highly viscous mantle material still keeps moving back to under the former ice shields, thereby creating a land uplift that amounts up to 2 cm/year. Neighbouring areas – in global terms – keep subsiding and seem to be sinking.
Today, the land uplift is most present in Fenno-Scandinavia and Northern parts of Canada. Present-day ice melting in areas such as Greenland and Svalbard adds elastic effects. It is therefore particularly important to consider post-glacial rebound for the cases discussed in Sections 4.2 and 4.3.

[2]Copyright permission granted by Rüdiger Haas (OSO) for use of the figure in this thesis.

3

On the S/X and VGOS telescopes

This chapter presents a short overview of the technical properties of both the S/X and VGOS telescopes, as well as the respective networks. The IVS network stations and cooperating sites displayed in Fig. 3.1 are stations of the S/X network.

3.1 The S/X equipment and network

S/X antennas have diameters ranging from 6 to 100 m and their slew speeds vary greatly between 0.3 and 3 deg/s (Elosegui, 2021). The frequencies used are 2.2 — 2.35 GHz (S-band) and 8.2 – 8.95 GHz (X-band) (Petrachenko, 2008). The circular polarised receivers and connected backends work at a recording rate ranging between 128 and 1024 Mbps, and the signal is sampled with 1 – 2 bit per sample for the majority of S/X experiments. Nowadays, the data are mostly stored on flexbuffs and then transferred electronically to the appointed correlation centre. Only few stations still record on disks called Mk5 or Mk6 modules that need to be shipped to the correlator. For scheduling standard experiments such as the R1, there is a determined source catalog[1] containing more than 300 sources (Thomas et al., 2024), however the selection of sources changes for every session.

3.2 The VGOS equipment and network

The VGOS antennas are mostly 12 – 13 m in diameter and slew at 6 – 12 deg/s in azimuth, 6 deg/s in elevation. The stations are equipped with broad band receivers that should cover 2 – 14 GHz according to the VGOS specifications, however, practically there are small deviations from this range at individual observatories (Petrachenko, 2006, 2008). The signal is recorded as dual-linear polarised and sampled with 2 bits/sample. The standard recording rate of VGOS stations is 8 Gbps Elosegui (2021). Again, most stations are capable of e-transferring the data, however, some still ship the disks. The increased slew and recording rates (compared to legacy S/X) result in a much higher number of scans per hour, e. g. up to 100 for the case of intensive sessions (Schartner et al., 2023). This enables faster and denser sampling of the atmosphere, which is recognized as one of the biggest error sources as discussed in section 2.5.3. For VGOS experiments, the source catalog

[1] "source.cat.geodetic.good" at `https://github.com/nvi-inc/sked_catalogs/`

[2] `https://ivscc.gsfc.nasa.gov/stations/ns-map.html`, 18 April 2024

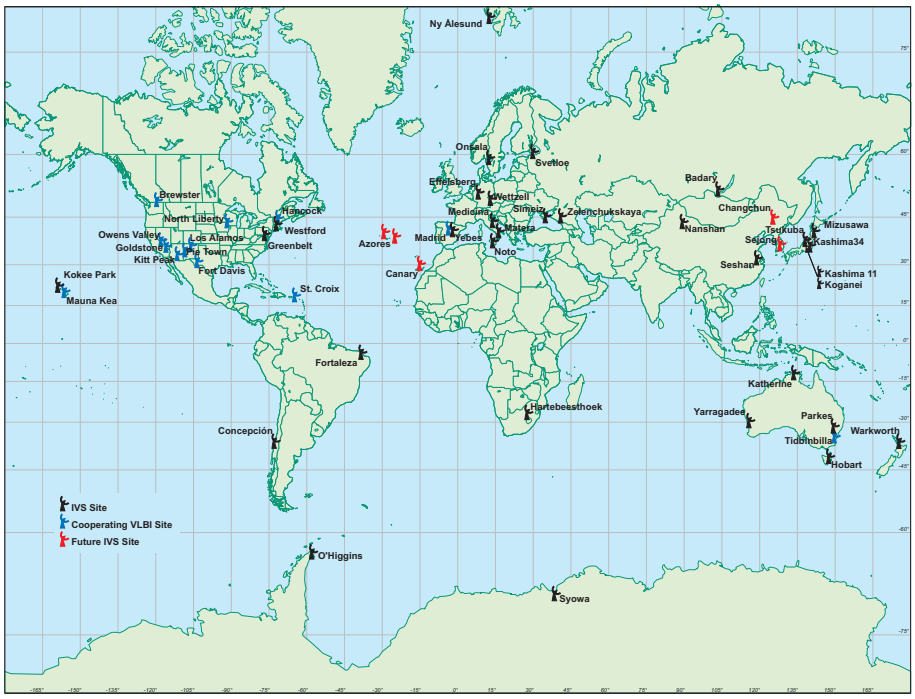

Figure 3.1: Map of the IVS network stations and cooperating sites[2].

used for scheduling is the same as for the S/X R1 and R4 experiments, while the VR (research and development) tend to explore a larger catalog of sources.

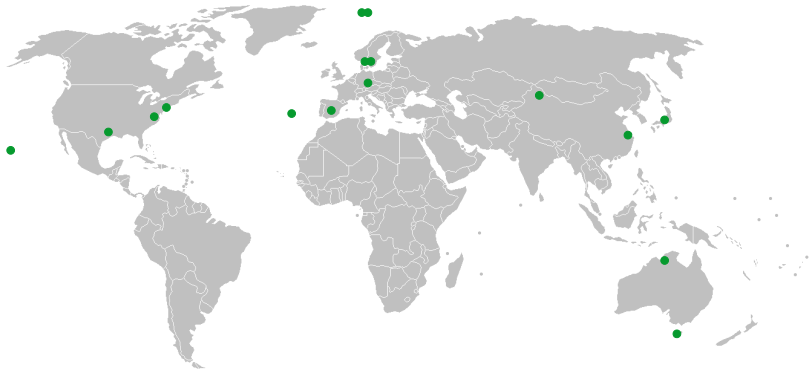

Figure 3.2: Map of the VGOS network as of February 2024.

4

Local ties

4.1 Background information

Chapter 3 describes two different networks for geodetic VLBI: S/X and VGOS. For operational experiments, individual telescopes from these networks are not usually scheduled together and therefore do not jointly perform observations. However, VGOS is expected to take over the tasks of the S/X network completely in the future. This is the main challenge that needs to be addressed. To avoid losing the reference to the decades of data that we have from S/X, it is necessary to connect the networks with each other.
Niell et al. (2021) and Varenius et al. (2021) were the first to publish papers in 2021 on local-tie measurements at their respective observatories in Kokee and Onsala, which were measured exclusively with radio interferometry instead of GNSS and engineering geodetic methods.

When observing with both telescope generations, the S/X equipment is often the limiting factor due to the more limited frequency range compared to the broadband receivers of the VGOS equipment. Additionally, the rotation rate of the newly build telescopes for the VGOS generation far outshines that of the old S/X telescopes, resulting in increased idle time.

There are two ways to initiate local-tie observations with S/X and VGOS: either by performing dedicated experiments or by joining all the telescopes to existing IVS experiments.
The first option encompasses that one does all the necessary tasks oneself, including scheduling, observing, correlating, and analyzing. This allows for the freedom to design and adapt everything according to one's needs. One can choose the frequencies that best suit the local Radio-Frequency Interference (RFI), for example. The observation time and experiment duration can be selected freely, and the weightings of individual parameters can be set specifically during scheduling. Additionally, the source catalogue is also under one's own control.
With the second option, at least some of the steps mentioned above are dispensable: The schedule already exists in full, and is readily available for download and can be processed as usual. In IVS experiments, the choice of e. g. observation frequencies is only available to a limited extent as it is necessary to find the best combination of frequencies that is favourable for the entire network. When joining IVS experiments,

it is preferable to tag along[1] telescopes with VGOS equipment to S/X sessions rather than the other way around, due to each generation's capability of observing established frequencies: VGOS equipment is intended for broad band observations in the range of 2–14 GHz, while the legacy equipment only covers S and X-band ranges at 2.2–2.35 and 8.2–8.95 GHz as mentioned in section 3.1. In any case, changes in the station's local hardware and software configurations may be necessary prior to observation in order to be able to record at the desired frequencies and recording rate.

Following the experiment, the correlation and analysis depend on whether one was officially involved in the tag-along mode or whether one joined in privately, so to speak. In the case of the official tag-along, correlation and analysis are carried out by the appointed IVS correlation and analysis centres. However, it should be noted that this is not the complete truth, as described in more detail in section 4.3.
Tag-alongs are particularly suitable when the time series of dedicated local-tie experiments is sparse or when there is no time for additional sessions. This may be the case when other researchers, such as astronomers, are also using the same antennas. Tag-alongs provide easier access for those with little experience in scheduling, correlation, or post-correlation.
The disadvantage of tag-alongs is that these experiments are generally optimised for a global network. This means that the choice of frequencies may not be adapted to locally known RFI, and that less scans are conducted than in dedicated local experiments. The latter is due to idle time while waiting for other stations or the distribution of co-located telescopes into different subnets. It is also important to note that these experiments are not intended for analyzing very short baselines. As a consequence, the correlators may not always spend a lot of effort on getting good delays for the short baselines. The tag-along NYTIEs showed that for these sessions, it is necessary to resolve phase ambiguities and identify outliers before obtaining useful results for further evaluation.

According to the VGOS standard, local-tie experiments can be observed using both S- and X-band frequencies, however, not all VGOS stations may actually be capable of observing also S-band. Fortunately, observing only on X-band is sufficient on such short baselines. The basic principle of local-ties is the very short baseline, i.e. one can actually assume the same influence of the ionosphere on the telescopes involved. Also, since the bandwidth of X-band is larger this is preferable over S-band.

[1]Note that "tagging along" in this thesis and the appended papers refers to a case in which a telescope is added to an experiment without having been considered during the scheduling process. Instead, the telescope may either be added officially at a later step by the scheduler, or in the case of co-located telescopes, one telescope may simply mirror the other's schedule. The only preconditions for successful tag-along are the mutual visibility of sources, and the technical properties of the telescope that need to match the observation mode and frequencies of the original schedule.

4.2 ONTIE

The ONTIE project involves experiments with the Onsala Space Observatory's geodetic VLBI antennas ONSALA60, ONSA13NE and ONSA13SW to determine the coordinates of the twin telescopes ONSA13NE and ONSA13SW and their respective baselines with respect to ONSALA60.
ONSALA60 (hereafter On) is a legacy S/X telescope with a receiver for right-handed circular polarised (rcp) signals. The diameter of the antenna is 20 m. It has been involved in geodetic VLBI observations since 1980. The ONSA13NE (Oe) and ONSA13SW (Ow) twin telescopes are VGOS telescopes with 13.2 m diameter. They are equipped with linearly polarised signal receivers operating within the range of 2 – 14 GHz and 3 – 15 GHz, respectively. This creates an overlap with On's frequency range within 8 – 9 GHz. They became operational in geodetic VLBI observations in 2019. The baselines On–Oe and On–Ow have a length of approximately 500 m each, while Oe and Ow are separated by about 75 m.
Dedicated short-baseline experiments between the three telescopes On, Oe, and Ow are referred to as ONTIE. They usually last 24 hours and the catalogue of the IVS operational VGOS series serves as the radio source catalogue. They are scheduled, observed, correlated and analysed at OSO. A total of 6 different frequency setups have been used since the first ONTIE experiments in 2019. Since February 2023, we have also internally tagged along Oe and Ow to IVS sessions such as R1 and RDV in which On regularly participates. Scheduling On was done by the IVS and Oe and Ow mirrored the schedule file, but correlation and analysis for the Onsala telescopes are handled by OSO. The data collected by Oe and Ow was not sent to the IVS.
First results were published by Varenius et al. (2021), and updates are presented in Paper I (presented at the 12th IVS General Meeting 2022) and also at the 26th European VLBI Group for Geodesy and Astrometry (EVGA) Working Meeting 2023 by Handirk et al. (2024).

Figure 4.1: Radio telescopes at OSO used for ONTIEs: the legacy S/X telescope ONSALA60 (radome, top right corner) and the VGOS twin telescopes ONSA13NE and ONSA13SW[2].

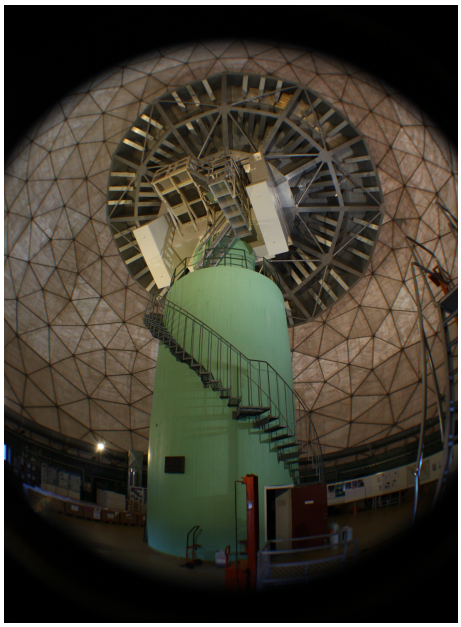

Figure 4.2: Inside the radome at OSO: the 20 m-antenna[3].

4.3 NYTIE

Since 1994, the GEON (Garcia-Espada et al., 2023) has been participating in VLBI experiments with the legacy S/X telescope NYALES20 (Ny). Since 2020 and 2022, respectively, the VGOS telescopes NYALE13S (Ns) and NYALE13N (Nn) have also been officially observing for the IVS.

Ny was an az-el mount legacy S/X telescope with a prime-focus antenna of 20 m diameter, designed for observations on S- and X-band for rcp signals. Its backend was a DBBC2 and data were recorded on a Mark 5B+. The telescope was dismantled in August 2023.
Ns and Nn are az-el mount VGOS telescopes with a ringfocus antenna of 13.2 m diameter. Their data are recorded on Flexbuff systems. However, Ns currently has legacy receiver equipment for S and X band for rcp signals. The backend is a DBBC2. Nn is equipped as a regular VGOS telescope with a frequency range from 2 to 14 GHz with vertical and horizontal polarisation, and the backend is a DBBC3. The baselines between Ny and Nn resp. Ns were about 1.5 km resp. 1.6 km, while Nn and Ns are about 85 m apart.
At GEON, a preliminary approach was taken to tag-along Ns to Ny in IVS R1-sessions. Kirkvik et al. (2021) reported very preliminary results. However, most experiments suffered from technical failures such as malfunctioning recording systems, malfunctioning elevation encoders, or a warm receiver. Therefore, further attempts were necessary.
Dedicated NYTIE sessions took place from March 2022 until the legacy antenna Ny

[2]Copyright permission granted by Roger Hammargren (OSO) for use of the photo in this thesis.
[3]Copyright permission granted by Mikael Lerner (OSO) for use of the photo in this thesis.

was dismantled and ceased operations in August 2023. A total of 23 short-baseline local interferometry campaigns, each lasting 24 hours, were conducted using the telescopes Ns and Ny, with Ny serving as the reference station in each case. Since March 2023, 9 experiments have also involved Nn.
Additional data were collected by adding Ns and Nn to regularly scheduled S/X IVS experiments with Ny. This addition was initially made for testing purposes of the Ns telescope. However, the results can also be used to analyse the local tie vectors at Ny-Ålesund. A selection of 33 R1, R4, RD and RDV experiments from these sessions are used to complement the dedicated NYTIE time series. These experiments are referred to as TA (tag-along) to distinguish them from the actual NYTIEs. More details are available in the Paper II.

(a) The former legacy S/X telescope NYALES20, dismantled August 2023.

(b) The new telescopes NYALE13N (VGOS equipment), left, and NYALE13S (S/X equipment), right.

Figure 4.3: Radio telescopes at GEON used for NYTIEs[4].

[4]Copyright permission granted by Susana Garcia Espada (GEON) for use of the photos in this

4.4 Comparison to tie measurements from GNSS and total station

To compare with the results obtained from radio interferometry local ties, tie vectors between the telescopes can also be measured using engineering geodetic methods. This includes both the classic measurements with total station as well as with GNSS. If the telescopes are designed accordingly, measurements can be set up directly in the azimuth cabin and taken from there to the outside or from the outside to the inside. This is the case in Ny-Ålesund, for example. If the azimuth cabin is not freely accessible, reflectors can be attached to the moving parts of the telescopes, such as the cabin or counterweights, instead. This allows for the calculation of the reference point of the telescope, which – in simplified terms – is the virtual intersection of the azimuth and elevation axes. Nothnagel (2008) discusses more details about the refence point. In Onsala, the S/X telescope poses an additional challenge due to its limited accessibility within the radome.

For both the ONTIEs and the NYTIEs, such measurements from the total station and GNSS are available, but the evaluation and comparison had not yet been completed at the time this thesis was finalised. Therefore, the thesis does not present the results.

thesis.

5

Summary

This thesis discusses the connection of co-localised radio telescopes with VLBI. Concrete examples of this are the ONTIE experiments at the Onsala Space Observatory and the NYTIE experiments at the Geodetic Earth Observatory Ny-Ålesund. In both cases, VGOS twins were added to the observatories that each already operated an S/X telescope in the late 2010s. Ns, one of the twins in Ny-Ålesund, is an exception as only the telescope construction represents the VGOS generation. However, the electronic equipment, including the receiver and backend, is currently still from the S/X generation.
At both observatories, the tie vectors between the old and new telescopes were determined using interferometric measurements on the short baselines. This allowed for the geometric establishment of the relationship between the data from the old and new antennas.

5.1 Summary of Paper I

The paper "Obtaining Local-Tie Vectors from Short-Baseline Interferometry" describes the implementation and evaluation of the ONTIE experiments, and is a continuation of the first publication on ONTIEs by Varenius et al. (2021).
The paper discusses the scheduling of the experiments in more detail and analyses and justifies the choice of observation frequencies. The evaluation includes both group and phase delay results, and reference is made to the possible influence of a faulty mechanical component on the measurement results.

5.2 Summary of Paper II

The paper "Obtaining Local-Tie Vectors from Short-Baseline Interferometry between legacy S/X and VGOS Telescopes at Ny-Ålesund" describes the implementation and evaluation of the NYTIE experiments.
This paper goes into more detail on the scheduling of the experiments and their evaluation. What is special about the NYTIEs is that the entire development and implementation of the project took place within about a year and a half under many unique circumstances: The project was created in spring 2022 under the assumption that the S/X telescope would be dismantled in spring 2023, i.e. there was high time pressure in some situations. This became particularly clear at the end of the active measurement phase of the project in spring and summer 2023. At the same time,

the project also suffered from repeated failure of the instrumentations.
In contrast to the ONTIE project, the NYTIE project can be considered completed, as the S/X telescope no longer exists since August 2023.
The paper presents the calculated local-tie vectors between the telescopes and also discusses the differences between dedicated experiments and the use of tag-along to existing IVS experiments.

Bibliography

Agnew, D. C. (2007). Earth Tides. In Herring, T. A., editor, Treatise on Geophysics: Geodesy, pages 163–195. Elsevier, New York.

Anderson, J. M. and Xu, M. H. (2018). Source Structure and Measurement Noise Are as Important as All Other Residual Sources in Geodetic VLBI Combined. Journal of Geophysical Research: Solid Earth, 123:162–190.

Artz, T., Halsig, S., Iddink, A., and Nothnagel, A. (2016). ivg::ASCOT: Development of a New VLBI Software Package. In IVS 2016 General Meeting Proceedings "New Horizons with VGOS". Johannesburg, South Africa.

Artz, T., Springer, A., and Nothnagel, A. (2014). A complete VLBI delay model for deforming radio telescopes: the Effelsberg case. Journal of Geodesy, 88(12):1145–1161. Web document `https://doi.org/10.1007/s00190-014-0749-1`.

Böhm, J. and Schuh, H. (2004). Vienna mapping functions in VLBI analyses. Geophysical Research Letters, 310:277–281.

Clivati, C., Ambrosini, R., Artz, T., Bertarini, A., Bortolotti, C., Frittelli, M., Levi, F., Mura, A., Maccaferri, G., Nanni, M., Negusini, M., Perini, F., Roma, M., Stagni, M., Zucco, M., and Calonico, D. (2017). A VLBI experiment using a remote atomic clock via a coherent fibre link. Scientific Reports, 7(1):40992. Web document `https://doi.org/10.1038/srep40992`.

Deutsches GeoForschungsZentrum (2019). ESMGFZ Product Repository - Elastic Surface Loading. `http://rz-vm115.gfz-potsdam.de:8080/repository/entry/show?entryid=24aacdfe-f9b0-43b7-b4c4-bdbe51b6671b`.

Elosegui, P. (2021). VLBI/VGOS Basics. TOW 2021: 11th IVS Technical Operations Workshop; Web document `https://www.haystack.mit.edu/wp-content/uploads/2021/05/TOW2021_Elosegui.pdf`.

Garcia-Espada, S., González, R. B., and Grinde, G. (2023). Ny-Ålesund Geodetic Observatory. In Armstrong, K. L., Behrend, D., and Baver, K. D., editors, International VLBI Service for Geodesy and Astrometry 2021+2022 Biennial Report, pages 73–76. NASA/TP-20230014975.

Gipson, J. (2018). Sked VLBI Scheduling Software User Manual. Web document `https://ivscc.gsfc.nasa.gov/IVS_AC/sked_cat/SkedManual_\v2018October12.pdf`.

Handirk, R., Varenius, E., Nilsson, T., Haas, R., le Bail, K., Meldahl, A., Wennesland, S. A. G., Gansmoe, T., González, R. B., and Garcia-Espada, S. (2024). Obtaining Local-Tie Vectors from Short-Baseline Interferometry between legacy S/X and VGOS Telescopes.

Hofmann-Wellenhof, B., Lichtenegger, H., and Wasle, E. (2008). GNSS – Global Navigation Satellite Systems. GPS, GLONASS, Galileo, and more. Springer Vienna.

Kallunki, J., Hase, H., and Zubko, N. (2023). Spectrum Management for the VLBI Global Observing System(VGOS) Observations. In International VLBI Service for Geodesy and Astrometry General Meeting 2022 Proceedings.

Kellermann, K. I., Bouton, E. N., and Brandt, S. S. (2020). A New Window on the Universe. In Open Skies: The National Radio Astronomy Observatory and Its Impact on US Radio Astronomy, pages 1–34. Springer International Publishing, Cham.

Kirkvik, A.-S., Dähnn, M., and Fausk, I. (2021). First results from the new station NYALE13S. In Haas, R., editor, Proceedings of the 25th European VLBI Group for Geodesy and Astrometry Working Meeting, pages 115–119. Web document `https://www.oso.chalmers.se/evga/25_EVGA_2021_Cyberspace.pdf`.

Landskron, D. and Böhm, J. (2018). VMF3/GPT3: refined discrete and empirical troposphere mapping functions. Journal of Geodesy, 92(4):349–360.

Lerner, M. (2012). Populärt om astronomi. Onsala rymdobservatorium, 3 edition.

Martí-Vidal, I., Roy, A., Conway, J., and Zensus, A. J. (2016). Calibration of mixed-polarization interferometric observations. Tools for the reduction of interferometric data from elements with linear and circular polarization receivers. Astronomy Astrophysics, 587.

Niell, A. E., Barrett, J. P., Cappallo, R. J., Corey, B. E., Elosegui, P., Mondal, D., Rajagopalan, G., Ruszczyk, C. A., and Titus, M. A. (2021). VLBI measurement of the vector baseline between geodetic antennas at Kokee Park Geophysical Observatory, Hawaii. Journal of Geodesy, 95(6):65. Web document `https://doi.org/10.1007/s00190-021-01505-9`.

Nilsson, T. and Haas, R. (2010). Impact of atmospheric turbulence on geodetic very long baseline interferometry. Journal of Geophysical Research: Solid Earth, 115.

Nothnagel, A. (2008). Conventions on thermal expansion modelling of radio telescopes for geodetic and astrometric VLBI. Journal of Geodesy, 83(8):787–792. Web document `https://link.springer.com/article/10.1007/s00190-008-0284-z`.

Nothnagel, A., Artz, T., Behrend, D., and Malkin, Z. (2017). International VLBI Service for Geodesy and Astrometry. Journal of Geodesy, 91(7):711–721. Web document `https://link.springer.com/article/10.1007/s00190-016-0950-5`.

Nothnagel, A., Holst, C., and Haas, R. (2019). A VLBI delay model for gravitational

deformations of the Onsala 20 m radio telescope and the impact on its global coordinates. Journal of Geodesy, 93(10):2019–2036. Web document https://link.springer.com/article/10.1007/s00190-019-01299-x.

Petit, G. and Luzum, B. (2010). IERS Conventions 2010. IERS Technical Note, (36). Frankfurt am Main: Verlag des Bundesamts für Kartographie und Geodäsie.

Petrachenko, B. (2006). VLBI2010 Antenna Specifications. IVS Memorandum 2006-022v01; Web document https://ivscc.gsfc.nasa.gov/publications/memos/ivs-2006-022v01.pdf.

Petrachenko, B. (2008). VLBI2010 Frequency Considerations. IVS Memorandum 2008-015v01; Web document https://ivscc.gsfc.nasa.gov/publications/memos/ivs-2008-015v01.pdf.

Schartner, M. (2021). VieSched++ VieVS VLBI Scheduling Software. Web document https://github.com/TUW-VieVS/VieSchedpp.

Schartner, M., Petrov, L., Plötz, C., Lemoine, F. G., Terrazas, E., and Soja, B. (2023). VGOS VLBI Intensives Between macgo12m and wettz13s for the Rapid Determination of UT1-UTC. In International Association of Geodesy Symposia, pages 1–6. Springer Berlin Heidelberg, Berlin, Heidelberg. Web document https://doi.org/10.1007/1345_2023_222.

Sovers, O. J., Fanselow, J. L., and Jacobs, C. S. (1998). Astrometry and geodesy with radio interferometry: experiments, models, results. Reviews of Modern Physics, 70(4):1393–1454. Web document https://arxiv.org/abs/astro-ph/9712238.

Takahashi, F., Kondo, T., Takahashi, Y., and Koyama, Y. (2000). Wave Summit Course: Very Long Baseline Interferometer. Ohmsha, Ltd. and IOS Press, Amsterdam, The Netherlands.

Thomas, C. C., MacMillan, D. S., and le Bail, K. (2024). Performance of the IVS R1 and R4 sessions. Advances in Space Research, 73(1):317–336. Web document https://www.sciencedirect.com/science/article/pii/S0273117723005550.

Varenius, E., Haas, R., and Nilsson, T. (2021). Short-baseline interferometry local-tie experiments at the Onsala Space Observatory. Journal of Geodesy, 95(5). Web document https://arxiv.org/abs/2010.16214.

Varenius, E., Maio, F., Le Bail, K., and Haas, R. (2022). Broad band flux-density monitoring of radio sources with the Onsala twin telescopes. Experimental Astronomy, 54(1):137–155.

Zhang, T., Gordon, R. G., Mishra, J. K., and Wang, C. (2017). The malpelo plate hypothesis and implications for nonclosure of the cocos-nazca-pacific plate motion circuit. Geophysical Research Letters, 44(16):8213–8218.